Spontaneous polarization and piezoelectricity in polar molecular crystals

Ivo Borriello, Giovanni Cantele, Domenico Ninno, and Giuseppe Iadonisi
Coherentia CNR-INFM and Dipartimento di Scienze Fisiche, Università di Napoli "Federico II,"
Complesso Universitario Monte Sant'Angelo, Via Cintia, I-80126 Napoli, Italy
(Received 23 December 2008; revised manuscript received 17 February 2009; published 31 March 2009)

Molecular materials with a polar arrangement of the constituent dipoles are good candidates for exhibiting piezoelectric properties directly related to the strain-induced polarization. We assess, from first principles, the properties of the metal-organic molecular crystal (4-dimethylaminopyridyl)bis(acetylacetato)zinc(II) in presence of strain. The spontaneous polarization and the piezoelectric properties are studied by means of the modern theory of polarization. The cooperative interaction among molecular chains is shown to lead to a collective polarization enhancement effect. Some theoretical issues concerning the multivalued behavior of the Berry phase are also illustrated.

DOI: 10.1103/PhysRevB.79.125126 PACS number(s): 71.20.Rv, 77.84.Jd

I. INTRODUCTION

Piezoelectric materials have a key role in the technological industry. Their importance is due to their wide use in manufacturing resonators, filters, and sensors. Indeed, piezoelectrics may combine sensing function (for the conversion of mechanical energy into electricity) with actuating functions (for the conversion of electricity to mechanical energy). Piezoelectrics are usually ceramics but a new interest toward piezoelectric organic materials is growing up, caused by their low weight, flexibility, and chemical inertness. Typically, organic crystals showing piezoelectric properties are modular systems with a polar arrangement of the constituent dipolar units.[1] A special case is represented by molecular crystals resulting from a perfect polar assembly of molecular dipoles along a crystallographic axis. Simple "screw-shaped" metal-organic molecules, including vapor-deposited films,[2–4] have been found to show a dominant tendency toward such organization in the solid state. The metal-organic molecular crystal (4-dimethylaminopyridyl)bis(acetylacetato)zinc(II) (ZNDA) belongs to this family of compounds. A single-crystal study[2] showed that ZNDA belongs to the noncentrosymmetric orthorhombic space-group *Fdd*2; more significantly, the molecular organization is perfectly polar with all the molecules aligned parallel to the z axis, as clearly shown in Fig. 1. ZNDA is characterized by good thermal stability and transparency; moreover, it is found to be organized as uniaxially oriented crystallites in vapor-deposited thin films on glass substrate.[5]

In this paper an *ab initio* study of piezoelectricity in this new material is performed by means of the density-functional theory. We employ the modern theory of polarization to compute the spontaneous polarization and its related quantities. Quantitative assertions about the piezoelectric properties are carried out. A detailed analysis on the relationship between the molecular dipole moment and the investigated macroscopic properties of the crystal evidences a collective polarization enhancement effect. The latter is related to the intermolecular interactions along and orthogonally to the polar axis direction.

The paper is organized as follows. In Sec. II, we briefly review the formulation of the modern theory of polarization in terms of Berry phase (BP) calculation and summarize the computational details. In Sec. III, we discuss the results of our calculation relating the investigated macroscopic properties of the molecular crystal with the intermolecular interactions. Finally, in Sec. IV, some conclusions are drawn.

II. METHODOLOGY

A. Modern theory of polarization

For a finite system, the polarization is defined as the total dipole moment per unit volume:

$$\mathbf{P} = \frac{1}{V}\left[\sum_{\tau} q^{\tau}\mathbf{R}^{\tau} - e\int_{V}\mathbf{r}n(\mathbf{r})d\mathbf{r}\right], \tag{1}$$

where V is the volume of the sample, q^{τ} and $\mathbf{R}^{\tau}$ are the charge and the position of the τth ion, and e and $n(\mathbf{r})$ are the electron charge and density, respectively. The definition in Eq. (1) cannot be generalized for an infinite periodic crystal

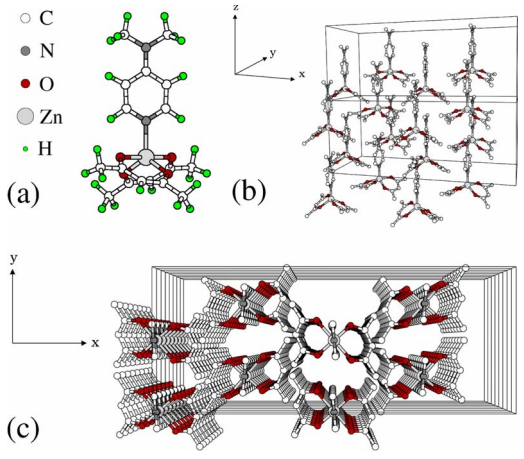

FIG. 1. (Color online) A schematic representation of the molecular ZNDA crystal. The screw-shaped molecules (shown in (a)) are disposed with the polar backbone aligned along the polar axis (as shown in (b)), giving rise to packed molecular chains (see (c)). The orthorhombic unit cell (black box) contains eight molecules, one per chain. In (b) and (c) H atoms are omitted for clarity.

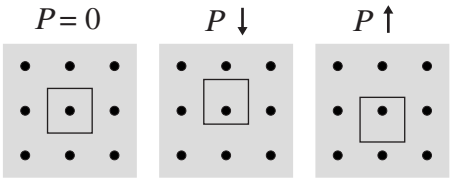

FIG. 2. Schematic representation of a two-dimensional system with periodically repeated cations (black circles) and uniform electronic charge density (gray). Different choices of the cell boundary correspond to different values of the dipole moment per unit cell [that is, of the polarization as defined in Eq. (1)]. On the contrary, the macroscopic polarization is expected to be zero by symmetry.

by replacing the sample volume with that of the unit cell because of the nature of the **r** operator. Indeed, in this way, the macroscopic polarization of a crystal would be defined as the dipole moment per unit cell and different choices of the lattice unit cell would yield to different values of P, which is unphysical. To better understand this point, a toy model is shown in Fig. 2.

Moreover, the measured quantities are generally variations in polarization, defined with respect to a reference configuration. This is the case of piezoelectricity (derivative of the polarization with respect to the applied strain) and spontaneous polarization in ferroelectrics (finite difference between two symmetric configurations in the hysteresis cycle). All these quantities are measured as bulk properties, whereas Eq. (1) leads to a polarization which depends on the truncation of the sample.

The modern theory of polarization (MTP) sheds light on how to define the polarization in crystalline dielectrics. The theoretical approach is described in detail in the papers by King-Smith and Vanderbilt[6] and by Resta;[7] here we only outline the main points.

The successful strategy for achieving a proper definition for the bulk crystal is to switch from a "charge" to a "current" description of the polarization variation. Within a finite system, the charge (the modulus of the wave function) is related to the current (the phase of the wave function) through the continuity equation (the variation in the charge at surface during a continuous transformation between two configurations is related to the current that flows in the bulk) so that both descriptions are equivalent. In an infinite crystal, this link is broken: the modulus and the phase of the wave function carry different information. In the MTP, the basic assumption is that the polarization variation is a property of the "current" and not of the "charge."

In the BP approach[6] of the modern theory, the total polarization is defined by

$$\mathbf{P} = \mathbf{P}^{\text{ion}} + \mathbf{P}^{\text{el}} = \frac{1}{V}\sum_{\tau} q^{\tau}\mathbf{R}^{\tau} + \sum_{n\text{occ}} \mathbf{P}^{(n)}, \tag{2}$$

with

$$\mathbf{P}^{(n)} = \frac{2ie}{(2\pi)^3}\int d\mathbf{k}\langle u_{n\mathbf{k}}|\nabla_{\mathbf{k}}|u_{n\mathbf{k}}\rangle, \tag{3}$$

where $u_{n\mathbf{k}}$ are the Block states of the system and n runs over all occupied bands. The value of **P** is obtained by computing the total geometric quantum phase

$$\phi_i = \frac{V}{e}\mathbf{G}_i \cdot \mathbf{P} = \frac{1}{e}\sum_{\tau} q^{\tau}\mathbf{G}_i \cdot \mathbf{R}^{\tau} + \frac{V}{e}\mathbf{G}_i \cdot \mathbf{P}^{\text{el}}, \tag{4}$$

where the phase ϕ_i is defined modulo 2π and $\mathbf{G}_i$ is the reciprocal-lattice vector in the ith direction[8] defined in such a way that $\mathbf{G}_i \cdot \mathbf{R}_i = 2\pi$ with $\mathbf{R}_i$ being a direct lattice vector. The first term is a lattice summation and the second one, known as "Berry phase," is computed from first principles. In practice, Eq. (3) is evaluated by summing over a discrete mesh of **k** points spanning the Brillouin zone. The total polarization in the ith direction is thus obtained as follows:

$$\mathbf{P}_i = \frac{1}{2\pi}\frac{e}{V}\phi_i\mathbf{R}_i. \tag{5}$$

The main result of the MTP is that the polarization $\mathbf{P}_i$ is now defined as a multivalued quantity (that is, modulo $e\mathbf{R}_i/V$). Nevertheless, the measurable quantity is the variation in polarization which instead corresponds to a well defined single-valued quantity. According to the MTP, the polarization difference between two configurations of a crystal can be evaluated provided that there exists a continuous transformation pathway connecting them, which keeps the system insulating.[7] The difference in total polarization (in the ith direction) $\Delta\mathbf{P}_i$ will be well defined if the change in the BP is accurately monitored along the configuration path connecting two states of the crystal.

To compute the spontaneous polarization of a crystal, a reference nonpolar configuration is needed (e.g., it could be obtained by symmetry considerations). In our case, the nonpolar configuration of the molecular crystal is obtained by alternately flipping molecules with respect to the polar axis ($i=3$ direction). In Fig. 3 a schematic representation of the transformation pathway we have chosen is shown, together with the computed values of the polarization along the path. The adopted strategy can be summarized as follows: (i) starting from the polar configuration, we have enlarged[9] the unit cell preserving the crystal symmetry (from zero to five); (ii) we have rotated one molecule for each two until the related dipole moment has been inverted (from 6 to 12); (iii) then, we have reduced the unit-cell volume down to its starting value (from 13 to 18).

The full circles in Fig. 3 represent the computed values of the polarization $\mathbf{P}_3$ at each configuration, whereas the empty circles are obtained from the former by adding an integer multiple of $e\mathbf{R}_3/V$. Indeed, a correct interpretation of the obtained data requires that the multivalued character of polarization is properly taken into account. Each computed value (full circles) is representative of a set of possible values of the polarization. Therefore, an infinite set of curves (often referred to as branches) represents the polarization as a function of the structural configuration along the continuous transformation pathway connecting the polar and the nonpolar states. Clearly two neighbor branches are separated, at each configuration, by $e|\mathbf{R}_3|/V$. We note that the computed values of polarization may belong to different branches. In order to reconstruct the branches, we discretized the transformation pathway in successive small structural variations in

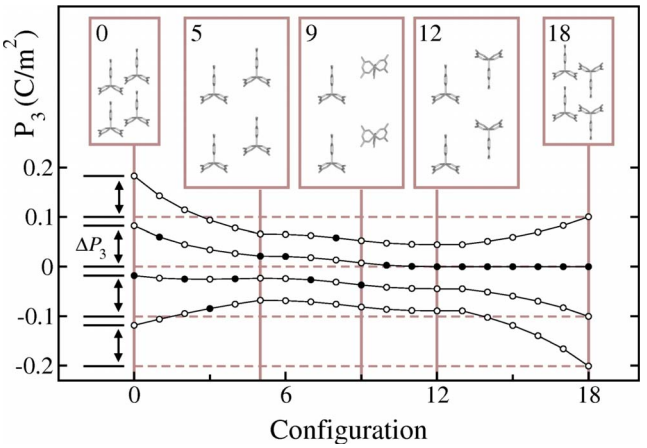

FIG. 3. (Color online) Scheme of the transformation pathway connecting the polar and nonpolar configurations of the crystal. Starting from the polar (zeroth) configuration, the unit cell is enlarged to increase the intermolecular distances. Then one molecule for each two is reverted to obtain a nonpolar configuration. The cell volume is then reduced down to its starting value. The computed values of polarization (full circles) are distributed on four branches. The polarization difference between the initial and the final states $\Delta\mathbf{P}_3$ does not depend on the choice of the branch. Its value is the spontaneous polarization value of ZNDA. The insets show the crystal configuration at some selected steps.

such a way that two consecutive values of $\mathbf{P}_3$ along the same branch verify the relation $|\Delta\mathbf{P}_3| \ll e|\mathbf{R}_3|/V$.

Figure 3 well summarizes both the multivalued character of the polarization and the branch independence of the polarization variation between the initial (zeroth) and final (18th) configurations. In general, the variation in polarization between two states of a crystal is branch independent only if the related multivalued polarizations are characterized by the same value of the modulus.

We stress that a detailed monitoring of the transformation pathway is essential to compute the spontaneous polarization. As shown in Fig. 3, it is not possible to evaluate the spontaneous polarization by considering only the polarization values at the initial and the final configurations: the relation $|\Delta\mathbf{P}_3| \ll e|\mathbf{R}_3|/V$ could be even misleading in this case.

The BP approach is employed to compute the piezoelectric properties as well. In the linear regime, the polarization changes induced by a small applied strain (about $\pm 1\%$) can be written as follows:

$$\delta\mathbf{P}_3 = e_{31}\mathbf{s}_1 + e_{32}\mathbf{s}_2 + e_{33}\mathbf{s}_3, \tag{6}$$

where e_{3i} are the piezoelectric stress constants, $\mathbf{s}_1=(a-a_0)/a_0$, $\mathbf{s}_2=(b-b_0)/b_0$, $\mathbf{s}_3=(c-c_0)/c_0$ are the strains along the x, y, and z axes, respectively, and a_0, b_0, c_0 are the values of the lattice parameters of the unstrained crystal. In our case we have computed the polarization for both the unstrained structure ($\mathbf{P}_3^{sp}$) and at several strained structures ($\mathbf{P}_3^S$), with equilibrium internal parameters determined at each strain value. The piezoelectric stress constants e_{3i} are directly obtained from the slope of the linear fit of the ($\mathbf{P}_3^S-\mathbf{P}_3^{sp}$) versus strain $\mathbf{s}_i$ curves, at small strains around the unstrained configuration.

B. Computational details

The calculations have been performed using a plane-wave pseudopotential approach based on the density-functional theory (DFT) as implemented in the QUANTUM-ESPRESSO package.[10]

We remark here that molecular crystals are mainly governed by intermolecular nonbonding interactions. Within DFT, an *ab initio* treatment of intermolecular binding is missing,[11] whereas no restrictions are posed when exploring the electronic properties at a fixed lattice structure.[12–14] Hence, the crystal structure has been computed by adopting the experimentally known space groups and lattice constants,[2] and relaxing the internal atomic coordinates.

Vanderbilt-type ultrasoft pseudopotentials[15] have been used with a plane-wave energy cutoff of 30 and 360 Ry for the electronic wave functions and the total charge density, respectively. The generalized gradient approximation with the Perdew-Burke-Ernzerhof parametrization[16] was employed for the evaluation of the exchange-correlation energy.

The polarization effects in the molecular crystal are compared with those of the isolated ZNDA molecules and of isolated molecular chains, in order to bring out enhancement or depolarization effects induced by interactions. Isolated molecules and molecular chains are treated by supercells. The minimum vacuum width separating periodic replica is about 22 Å for neighbor chains and about 17 Å for isolated molecules. In both cases an accurate convergence check of the vacuum region sizes confirmed that neighbor replica are separated enough to prevent spurious interactions between them. The Brillouin zone of the crystal was sampled using a $2\times2\times2$ Monkhorst-Pack[17] **k**-point grid while the density of states (DOS) has been computed on a $12\times12\times12$ **k**-point grid. The Γ-point specific algorithm has been used for supercells. The **k**-space integrations for the BP calculations has been made on a uniform $3\times3\times7$ **k**-point mesh. The convergence of all the results with respect to the number of **k** points and the plane-wave cutoff energy has been carefully tested.

III. RESULTS

A. Collective polarization effects

The ZNDA molecular crystal is composed by screw-shaped molecules with a dipolar backbone and a head group that curtails lateral interactions without obstructing the head-to-tail Coulombic interactions along the polar axis. This means that the intermolecular interactions do not involve chemical bond formation. As a consequence, it is expected that the electronic structure of the crystal is quite similar to that of the isolated molecule. In Fig. 4 the electronic DOS is shown for both the molecular crystal and the isolated molecule. The zero of energy is set at the middle of the band gap between occupied and empty states. The DOS reveals that the ZNDA band gap depends on the molecular electronic structure and is almost independent on the intermolecular distance. This result guarantees that the transformation pathway described in Fig. 2 keeps the system insulating, as required by the MTP.

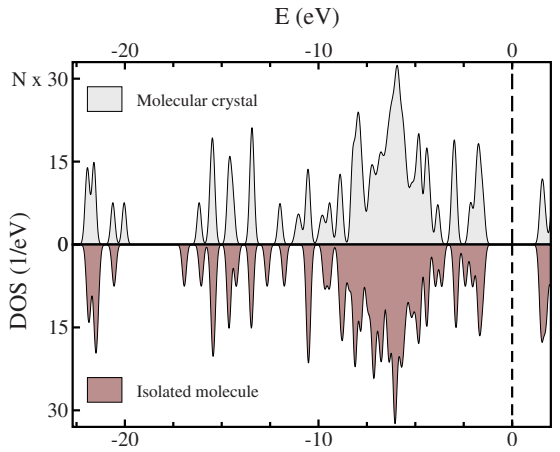

FIG. 4. (Color online) Calculated electronic properties of the ZNDA crystal and the isolated molecule. The zero energy is set at the middle of the band gap between filled and empty states. N is the number of molecules in the unit cell. The comparison between the total DOS evidences that the band gap does not depend on the intermolecular distance.

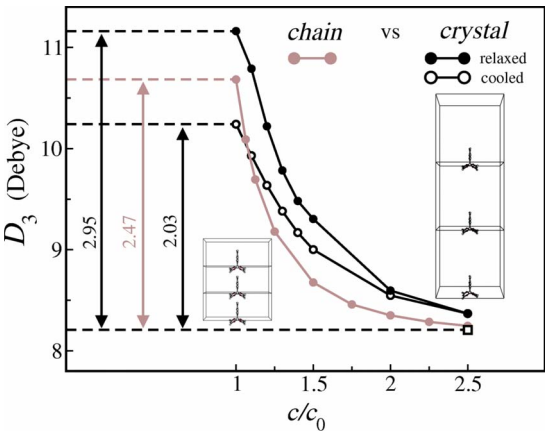

FIG. 5. (Color online) The dipole moment per molecule $\mathbf{D}_3$ as a function of the intermolecular distance along the chain. The lines are guides for eye. Two different systems are considered: isolated chains and crystals (cooled and relaxed). The latter can be viewed as systems of packed chains (see text). The insets show the molecular chain structure in correspondence of two different values of the ratio c/c_0.

As stated above, ZNDA crystallizes in an orthorhombic face-centered structure, space-group $Fdd2$, with half a molecule in the asymmetric unit; a C_2 rotation generates the other half. As a result, eight molecules are associated to the conventional unit cell [black box in Fig. 1(b)]: one for each chain [see Fig. 1(c)], characterized by the same structural conformation. Moreover, by symmetry, the molecular dipole moment is directed along the z axis (polar axis). This means that each molecule equally contributes to the total dipole density, that is, to the polarization of the crystal. The polarization can be thus rewritten in terms of single contributions as follows:

$$\mathbf{P}_3 = n\mathbf{D}_3, \tag{7}$$

where $n=N/V$ is the dipole unit density, N is the number of dipole units per cell, V is the cell volume, and $\mathbf{D}_3$ is the unitary dipole moment. Of course, the latter is the dipole moment associated to a single molecule. Equation (7) differs from Eq. (1): the latter is obtained from the charge distribution inside the unit cell, and thus it depends on the choice of the cell boundaries, the former depends only on the number of molecules associated with the unit cell, which is a well defined quantity ($N=8$ molecules per cell in ZNDA). A question to be addressed is what happens to the molecular dipole moment when molecules are arranged to form ZNDA crystal structure. In order to answer this question, some points must be taken into account: (i) the crystal can be viewed as a system of opportunely packed chains of molecules, as clearly shown in Fig. 1(c); (ii) the dipole moment of each molecule inside the crystal depends on both the intermolecular distance within the same chain and the interchain distance; (iii) the dipole variation can be decomposed into two contributions: the first associated with the molecular electronic charge at a fixed atomic configuration, and the second to the molecular structural relaxation. Three different cases have been thus considered: (i) crystals with fully optimized internal atomic positions (referred to as relaxed crystals); (ii) crystals with internal coordinates fixed so that each molecule has the same structural configuration of the isolated one (cooled crystals); (iii) isolated molecular chains with internal coordinates fixed so that each molecule has the same structural configuration of the isolated one.

Our analysis of the molecular dipole moment is shown in Fig. 5. For the crystal, the unit-cell volume has been enlarged keeping constant the ratio between lattice parameters, thus preserving the space-group symmetry $Fdd2$. In chains, a tetragonal supercell has been adopted with a square basis fixed at $a=b=2.5c_0$. The dipole moment was achieved through BP calculation of the polarization $\mathbf{P}_3$ and by using Eq. (7); the value of n is opportunely assigned for each system. As shown in Fig. 5, $\mathbf{D}_3$ has been studied as a function of the lattice parameter along the polar axis. At a fixed value of the ratio c/c_0 all the systems are characterized by the same intermolecular distance along the chains. The most relevant feature of the curves is a dramatic increasing of the dipole moment when molecules are brought out from the noninteracting limit and disposed at the crystallographic distance along the chains. In Fig. 5 the value of the dipole moment for the isolated molecule has also been reported (empty square). In this case, the dipole moment has been computed using Eq. (1) where V is the volume of the cubic supercell with $a=b=c=2.5c_0$. The crystal packing causes a raise of about 36% of the total dipole moment with respect to the isolated molecule, going from 8.21 to 11.16 D. By comparing the curves for cooled and relaxed crystals, the former case leads to nearly 70% of the total polarization enhancement, thus evidencing that the polarization increase is mainly ascribed to the electronic degree of freedom. This feature is also found in other organic piezoelectric crystals.[18] Interestingly, the comparison between the curves for isolated molecular chains and cooled crystals evidences that the interchain interaction at the experimental distances ($c/c_0=1$) lowers the polarization enhancement effect.

TABLE I. Spontaneous polarization and piezoelectric constants (in C/m^2) for ZNDA compared with those computed for the organic ferroelectric polymer crystal PVDF as reported in Ref. 20. Experimental lattice parameters are given in Å.

	a_0	b_0	c_0	P_3^{sp}	e_{31}	e_{32}	e_{33}
ZNDA	28.057	11.363	11.325	0.082	−0.070	−0.075	−0.145
PVDF				0.178	−0.268	−0.270	−0.332

B. Piezoelectric properties

The polarization variation as a function of the applied strain along the crystal axes is reported in Fig. 6. The negative value of the slopes is strictly connected to the nature of piezoelectricity in organic crystals. At variance with inorganic materials, organic piezoelectrics are modular systems constituted by opportunely packed dipole units (typically polymers or molecules). By reducing (increasing) the cell volume the dipole density will be higher (lower) leading to a negative value of the piezoelectric stress constants. In inorganic materials, piezoelectricity is instead mainly associated with ions displacement: in this case the piezoelectric constants can take even positive values and generally are higher in modulus with respect to those in organic counterparts.[19] Among organic piezoelectrics, polyvinylidene fluoride (PVDF) is the most known, studied, and used for its piezoelectric properties.[1] For this reason, to give a quantitative idea of the potential offered by ZNDA, we compare our results with that of PVDF. The spontaneous polarization and piezoelectricity in ZNDA are presented in Table I, together with that of PVDF as reported in Ref. 20. Our results evidence two different piezoelectric responses depending on the applied strain direction: (i) along the polar axis; (ii) in the plane orthogonal to it. To give an insight on this point, let us assume that the value of dipole moment unit does not change by applying small strains to the experimental crystal structure. By using Eq. (7), the polarization (indicated in this case with $\mathbf{P}_3^{cd}$) would thus depend on the strain modulus as follows:

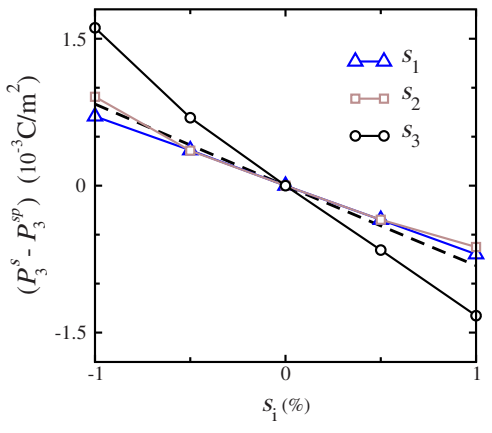

FIG. 6. (Color online) Polarization variation as a function of the strain. The dashed line is obtained from Eq. (9). Solid lines are guides for eyes.

$$\mathbf{P}_3^{cd}(s) = \frac{N}{a_0 b_0 c_0 (1+s)} \mathbf{D}_3^0 = \frac{1}{(1+s)} \mathbf{P}_3^{sp}, \tag{8}$$

where $\mathbf{D}_3^0$ is the dipole moment unit for the unstrained crystal and s is the strain modulus. In Fig. 6 the dashed curve represents the polarization variation in this "constant dipole" approximation whose analytic expression is easily written as

$$\mathbf{P}_3^{cd} - \mathbf{P}_3^{sp} = -\frac{s}{(1+s)} \mathbf{P}_3^{sp}. \tag{9}$$

As it is clearly shown in Fig. 6, the polarization variations related to applied strain along nonpolar crystal axes well agree with this model. On the other hand, polarization variation due to the applied strain along the polar axis is not fitted by Eq. (9), indicating that in this case the assumption of constant dipole moment unit does not hold. This means that, at variance with the intermolecular interaction along the chain, the role of interchain interaction is negligible in the piezoelectric response.

IV. CONCLUSIONS

In this work we have performed *ab initio* calculations in the framework of the MTP in order to characterize the spontaneous polarization and the piezoelectric response of ZNDA molecular crystal under an applied strain. We have computed the piezoelectric stress coefficients and compared our results to the most popular piezoelectric organic material, PVDF. Even if the piezoelectric moduli of ZNDA are lower, they are comparable with PVDF ones within the same order of magnitude. Our results show that molecules disposed in crystal configuration give rise to a collective polarization enhancement, mainly due to the intermolecular interaction along the polar axis direction. This property induces a relevant difference in piezoelectric response of ZNDA depending on the strain direction, as clearly shown by the values of piezoelectric coefficients relative to the strain along and orthogonal to the polar axis. This feature may be useful in technological applications where a dominant direction in piezoelectric response is requested.

ACKNOWLEDGMENTS

We acknowledge the financial support from the National PON Project "Sonar Tridimensionale Stereoscopico Simultaneo a 500 kHz" (Contract No. STSS-500). Calculations were performed at CINECA-Bologna ("Progetti Supercalcolo 2008") advanced computing facilities.

[1] See, for example, R. G. Kepler and R. A. Anderson, Adv. Phys. **41**, 1 (1992) and references therein.
[2] S. P. Anthony and T. P. Radhakrishnan, Chem. Commun. (Cambridge) (**2001**) 931.
[3] S. P. Anthony, P. Raghavaiah, and T. P. Radhakrishnan, Cryst. Growth Des. **3**, 631 (2003).
[4] S. P. Anthony, N. K. M. N. Srinivas, D. N. Rao, and T. P. Radhakrishnan, J. Mater. Chem. **15**, 739 (2005).
[5] S. P. Anthony, S. Porel, D. N. Rao, and T. P. Radhakrishnan, Pramana **65**, 871 (2005).
[6] R. D. King-Smith and D. Vanderbilt, Phys. Rev. B **47**, 1651 (1993).
[7] R. Resta, Rev. Mod. Phys. **66**, 899 (1994) and references therein.
[8] $i=1,2,3$ correspond, respectively, to x, y, and z directions, where z corresponds to the polar axis.
[9] Such step is needed in this specific case because some of the configurations (central panel, in the inset of Fig. 3) could not be achieved otherwise.
[10] URL: http://www.quantum-espresso.org.
[11] D. Nabok, P. Puschnig, and C. Ambrosch-Draxl, Phys. Rev. B **77**, 245316 (2008).
[12] M. L. Tiago, J. E. Northrup, and S. G. Louie, Phys. Rev. B **67**, 115212 (2003).
[13] K. Hummer, P. Puschnig, and C. Ambrosch-Draxl, Phys. Rev. Lett. **92**, 147402 (2004).
[14] G. Koller, S. Berkebile, M. Oehzelt, P. Puschnig, C. Ambrosch-Draxl, F. P. Netzer, and M. G. Ramsey, Science **317**, 351 (2007).
[15] D. Vanderbilt, Phys. Rev. B **41**, 7892 (1990).
[16] J. P. Perdew, K. Burke, and M. Ernzerhof, Phys. Rev. Lett. **77**, 3865 (1996).
[17] J. D. Pack and H. J. Monkhorst, Phys. Rev. B **16**, 1748 (1977).
[18] S. M. Nakhmanson, M. Buongiorno Nardelli, and J. Bernholc, Phys. Rev. B **72**, 115210 (2005).
[19] See, for example, G. Saghi-Szabo, R. E. Cohen, and H. Krakauer, Phys. Rev. Lett. **80**, 4321 (1998); L. Bellaiche and D. Vanderbilt, *ibid.* **83**, 1347 (1999).
[20] S. M. Nakhmanson, M. Buongiorno Nardelli, and J. Bernholc, Phys. Rev. Lett. **92**, 115504 (2004).